THE BELL SYSTEM TECHNICAL JOURNAL
Vol. 62, No. 4, April 1983
Printed in U.S.A.

Adaptive Linearization of Power Amplifiers in Digital Radio Systems

By A. A. M. SALEH and J. SALZ

(Manuscript received October 5, 1982)

High-frequency power amplifiers operate most efficiently at saturation, i.e., in the nonlinear range of their input/output characteristics. This phenomenon has traditionally dictated the use of constant envelope modulation methods for data transmission, resulting in circular signal constellations. This approach has inherently limited the admissible data rates in digital radio. In this paper we present a method for solving this problem without sacrificing amplifier power efficiency. We describe and analyze an adaptive linearizer that can automatically compensate for amplifier nonlinearity and thus make it possible to transmit multilevel quadrature amplitude modulated signals without incurring intolerable constellation distortions. The linearizer utilizes a real-time, data-directed, recursive algorithm for predistorting the signal constellation. Our analysis and computer simulations indicate that the algorithm is robust and converges rapidly from a blind start. Furthermore, the signal constellation and the average transmitted power can both be changed through software.

I. INTRODUCTION

Progress in high-speed data transmission over radio channels has lagged behind that of the voiceband channel. Inherent difficulties associated with implementing automatic equalizers are partially responsible, but the application of multilevel quadrature amplitude modulation (QAM) also has been inhibited by the amplitude (AM/AM) and phase (AM/PM) nonlinearities present in radio-frequency (RF) power amplifiers.

Recent work[1] has evolved design principles showing a possibility of substantial improvements in QAM performance over linear fading radio channels. A crucial obstacle to achieving these gains is the nonlinear distortion introduced by power amplifiers. Attempts to re-

alize high-speed data transmission over these channels force consideration of methods to cope with this nonlinear distortion.

One approach is to back off from saturation sufficiently so that the signal level is restricted to the linear range of amplification. The required amount of power back-off can be several decibels, resulting in an inefficient operation of the power amplifier. Moreover, the achievement of a given desired level of average transmitted power would require the use of a large, expensive, and high-power-consuming amplifier.

It has been realized[2-7] that some improvements in this regard can be obtained by using fixed signal predistortion circuits prior to amplification. Such circuits, however, cannot compensate for drifts in power amplifier nonlinearities caused by temperature changes, dc power variations, and component aging. These fluctuations can considerably degrade performance of systems employing constellations with large numbers of points, say 64 or higher, and the use of an adaptive technique is necessary in these applications.

Conceptually, the nonlinear distortion introduced by the power amplifier can be minimized at the receiver by an adaptive nonlinear equalizer. Such schemes have been proposed and studied in voiceband data transmission[8] and for filtered PSK signals operating over satellite channels.[9] This approach does not seem to be reasonable or necessary in our application, since the source of the nonlinearity is at the transmitter. Thus, it would appear logical to equalize the nonlinearity at the transmitter, where it occurs and where the transmitted bits are available.

Thus, this paper focuses on the problem of adaptive predistortion linearization. We describe a transmitter-based recursive algorithm for predistorting the signal constellation, thereby rendering a virtually linear transmitter. The algorithm operates in real time and is data directed. The predistortion is accomplished within a digital memory, which is used to generate the desired baseband signal. This maximizes the use of digital technology, and increases the reliability and flexibility of the system. For example, it is possible to change the signal constellation and the average transmitted power through software. Our treatment applies only to single-valued, memoryless nonlinearities.

The idea of adaptive predistortion of signal constellations has been previously suggested.[10] In this reference, the predistortion of each point of the constellation is accomplished by switching the RF or intermediate-frequency (IF) input signal to a separate path containing an adjustable diode attenuator and an adjustable diode phase shifter. The analog hardware required for such an implementation would be quite involved, especially for a large number of points. We have also found in the patent literature[11] a description of a digital adaptive

predistorter that appears to be similar to the one we present here. However, no detailed description of the algorithm or its behavior is provided.

Our basic ideas are described in Section II. Mathematical analysis is provided in Section III, and simulation results of the adaptive linearizer with finite-precision arithmetic are given in Section IV.

II. GENERAL DESCRIPTION AND REQUIREMENTS OF OPERATION

A block diagram of a QAM transmitter with the proposed predistortion linearizer is shown in Fig. 1. A random access memory (RAM) contains the predistorted values of the in-phase and quadrature voltages of each point on the QAM constellation. A memory-lookup encoder obtains each input data symbol and generates the RAM addresses of the desired signal point. The corresponding stored, predistorted voltage values are converted to analog voltages using a pair of digital-to-analog (D/A) converters. These voltages drive a quadrature modulator, which generates the desired predistorted RF signal for the duration of the input symbol. That signal is then amplified, filtered, and transmitted. This part of the linearizer is similar in operation to a recently proposed memory-based encoder described in Ref. 12.

To update the RAM information, the amplifier output is sampled by a directional coupler and demodulated using the same local oscillator used for the modulator, which eliminates the need for carrier recovery. The output in-phase and quadrature voltages of the demodulator are converted to digital form using a pair of analog-to-digital (A/D) converters. A linearizing processor, which is the heart of the linearizer, receives this information, compares it with the input data, and computes the resulting error. A recursive algorithm, which is discussed in the next section, uses the error to update the voltage values in the RAM corresponding to the particular data point under consideration. Note that each point on the signal constellation is treated separately. Thus, the linearizer can support any desired constellation.

The memory-lookup encoder and the D/A converters have to operate, of course, at the full signaling rate. However, the linearizing processor and the A/D converters can operate at a much reduced rate, since the updating process is only needed to compensate for drifts that occur on a much slower time scale than the data rate.

We now emphasize a crucial point. The proper operation of the linearizer as described above assumes that the amplifier is memoryless, and requires that the signal not be filtered before the power amplifier. Thus, all pulse shaping and filtering must be performed by the combination of the post-amplifier, RF bandpass filter, and the receiver filters. The former filter should be designed just to meet FCC (or

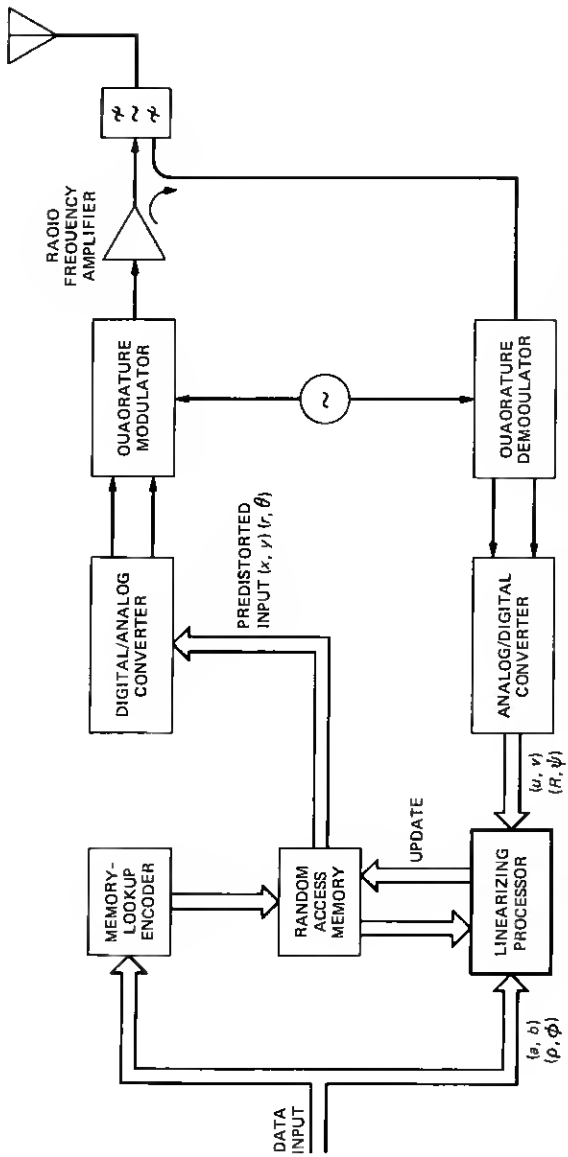

Fig. 1—Schematic representation of the adaptive, digital, predistortion linearizer.

other) emission rules for square input pulses, as described in Ref. 13. Such an implementation may require an automatic equalizer at the receiver to eliminate residual intersymbol interference. It was shown[1] that, even with ideal filtering, adaptive equalization would still be necessary to compensate for multipath fading using QAM signals with large numbers of levels. Thus, the elimination of pre-amplifier pulse shaping appears to be a mild constraint.

Because of the more stringent requirement on the post-amplifier, RF bandpass filter, its loss would of course be increased over that of the conventional case where preamplifier filtering does the spectrum shaping. However, computations[14] based on practical filters[15] operating in the 6-GHz band show that the RF filter loss would only increase from about 0.5 dB to 1.5 dB. However, we will see in Section IV that the linearizer in our system would allow the operation of the power amplifier to approach saturation. This would result in several decibels of power increase, which would more than compensate for the one-decibel increase in the filter loss.

III. THE RECURSIVE ALGORITHM

As we already mentioned, our approach is applicable to any signal constellation. However, for clarity of exposition, we restrict our analysis to a rectangular constellation. Referring to Figs. 1 and 2, we denote a point on the rectangular QAM constellation by the complex number

$$a + ib = \rho e^{i\phi},$$

where, for an L^2-level system, a and b assume values on the lattice $\pm 1 \pm 3 \pm 5 \pm \cdots \pm (L-1)$. We denote the predistorted point by the

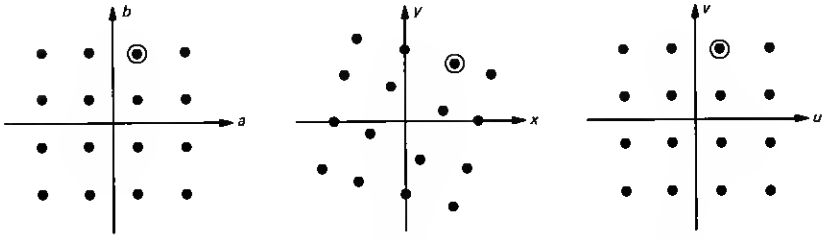

Fig. 2—The signal constellations at various points in the linearizer of Fig. 1. (a) Quadrature amplitude modulation data. (b) Digital/analog data. (c) Analog/digital data.

complex number

$$x + iy = re^{i\theta}.$$

A sequence of these points amplitude and phase modulates a carrier at frequency f_c and the resulting signal,

$$S(t) = \sum_m r^{(m)} p(t - mT) e^{i[2\pi f_c t + \theta^{(m)}]}, \tag{1}$$

is applied to the amplifier. In (1), $p(t)$ is a rectangular pulse, $1/T$ is the signaling rate, and $r^{(m)}$, $\theta^{(m)}$ represent the amplitude and phase of the mth data symbol.

The amplifier is customarily represented by a pair of memoryless nonlinear functions.[16,17] The amplitude function, $A(r)$, causes amplitude distortion (AM/AM) and the phase function, $\Phi(r)$, causes amplitude to phase conversion (AM/PM). Thus the signal, (1), after amplification becomes

$$S_o(t) = \sum_m A(r^{(m)}) p(t - mT) e^{i[2\pi f_c t + \theta^{(m)} + \Phi[r^{(m)}]]}. \tag{2}$$

Figure 3 shows sketches of typical curves $A(r)$ and $\Phi(r)$ for a traveling-wave tube (TWT) power amplifier.

We remark that if the functions $A(\cdot)$ and $\Phi(\cdot)$ were known exactly we could choose transformations $g(\cdot)$ and $h(\cdot)$ from points (ρ, ϕ) to

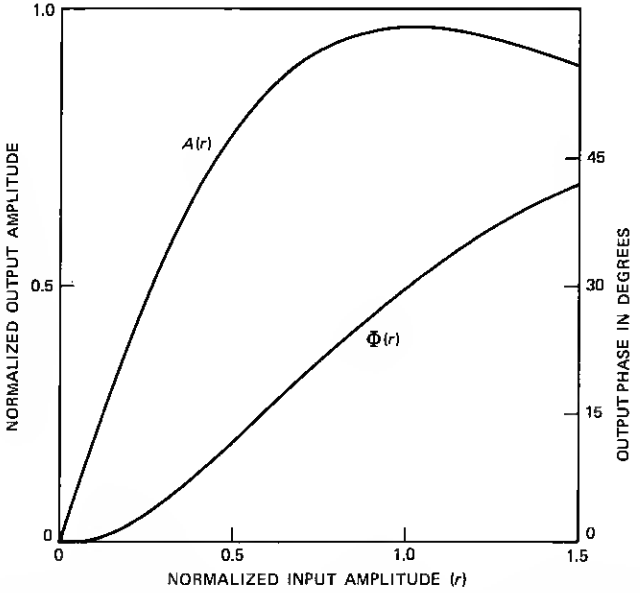

Fig. 3—Typical example of the input/output amplitude and phase characteristics of a TWT amplifier.

(r, θ) so that

$$A(r) = A[g(\rho)] = G\rho, \tag{3}$$

where

$$r = g(\rho)$$

and

$$\Phi(r) + h(\phi, \rho) = \phi + \zeta, \tag{4}$$

where

$$\theta = h(\phi, \rho).$$

The constant gain, G, in (3) is some desired gain, taking into account the linear gain of the power amplifier and the coupling factor of the sampling directional coupler. The fixed phase shift, ζ, in (4) is arbitrary and can be set to zero without loss of generality.

Finally, let the measured data point from the A/D converter be

$$u + iv = Re^{i\psi}.$$

The object of the predistortion is to find a solution

$$r = \hat{r}$$

and

$$\theta = \hat{\theta},$$

such that

$$Re^{i\psi} = G\rho e^{i\phi}. \tag{5}$$

We now describe an iteration procedure that converges to (5).

Since data are usually scrambled, a specific data point (ρ, ϕ) will occur at random. Let (r_n, θ_n) be the predistorted RAM data point and (R_n, ψ_n) be the measured data point at the nth time the desired data point (ρ, ϕ) occurs. The measured output radius R_n is then

$$R_n = A(r_n) + \nu_n \tag{6a}$$

while the measured angle is

$$\psi_n = \Phi(r_n) + \theta_n + \mu_n, \tag{6b}$$

where ν_n and μ_n are zero-mean measurement errors. If the measurements were perfect and noiseless, we would simply solve the following two nonlinear equations

$$f(\hat{r}) = A(\hat{r}) - G\rho = 0 \tag{7}$$

and

$$\Phi(\hat{r}) + \hat{\theta} - \phi = 0 \tag{8}$$

for $\hat{r}$ and $\hat{\theta}$.

A great number of iterative procedures are known for solving the nonlinear equations given in (7) and (8). In the presence of measurement noise (with convex functions A and Φ), stochastic approximation algorithms[18] provide efficient methods. So, if one chooses step sizes α_n and β_n, which behave as $o(1/n)$, the following recursions are known to converge to the true solutions $\hat{r}$ and $\hat{\theta}$ in a mean-square sense:

$$r_{n+1} = r_n - \alpha_n(R_n - G\rho) \tag{9a}$$

$$\theta_{n+1} = \theta_n - \beta_n(\psi_n - \phi). \tag{9b}$$

To provide a rationale for the above recursions we analyze, in some detail, the behavior of (9a). The behavior of (9b) is similar. Since $f(X)$, eq. (7), is continuous on $(X_0, X_{\max})$ and if, by hypothesis, the derivative $f'(X)$ of $f(X)$ exists on this interval, then there is a ξ such that

$$X_0 \le \xi \le X_{\max}$$

$$f'(\xi) = \frac{f(X_{\max}) - f(X_0)}{X_{\max} - X_0}. \tag{10}$$

Applying this mean-value theorem to $f(r_n)$, eq. (7), we get

$$f(r_n) = A(r_n) - G\rho = f(\hat{r}) + f'(\xi_n)(r_n - \hat{r}), \tag{11}$$

where ξ_n lies between r_n and $\hat{r}$. Substituting this into (9a) we get

$$r_{n+1} - \hat{r} = r_n - \hat{r} - \alpha_n[A'(\xi_n)(r_n - \hat{r}) + \nu_n]. \tag{12}$$

In (12) we made use of the fact that $f(\hat{r}) = 0$ and subtracted $\hat{r}$ from both sides of the equation.

Letting $\alpha_n A'(\xi_n) = \gamma_n$, $r_n - \hat{r} = \delta_n$ and then iterating (12) we obtain

$$\begin{aligned}\delta_{n+1} &= (1 - \gamma_n)\delta_n - \frac{\gamma_n \nu_n}{A'(\xi_n)} \\ &= \delta_1 \prod_{i=1}^{n} (1 - \gamma_i) - \sum_{k=1}^{n} \frac{\nu_k}{A'(\xi_k)} \frac{\gamma_k}{1 - \gamma_k} \prod_{i=k}^{n} (1 - \gamma_i).\end{aligned} \tag{13}$$

We now compute the mathematical expectation of δ_n and the variance:

$$\begin{aligned}\bar{\delta}_{n+1} = E\{\delta_{n+1}\} &= E\{\delta_1\} \prod_{i=1}^{n} (1 - \gamma_i) \\ &\le E\{\delta_1\} e^{-\sum_{i=1}^{n} \gamma_i}\end{aligned} \tag{14}$$

and

$$\sigma_{n+1}^2 = E\{\delta_{n+1} - \bar{\delta}_{n+1}\}^2 = \sigma_\nu^2 \sum_{k=1}^{n} \frac{\gamma_k^2}{[A'(\xi_k)]^2(1 - \gamma_k)^2} \prod_{i=k}^{n} (1 - \gamma_i)^2, \tag{15}$$

where $\sigma_\nu^2 = E\{\nu_n^2\}$. We see from (14) and (15) that rapid convergence of the algorithm is critically dependent on the step-size sequence, γ_n, which in turn depends on the derivative of the nonlinearity in the neighborhood of the solution. While the derivative is unknown, in most applications it can be bounded away from zero and this makes it possible to estimate the best step-size sequence. We see from (14) that, even in the absence of noise, the algorithm is guaranteed to converge to the true solution only if the step-size series diverges, i.e.,

$$\sum_{i=1}^{n} \gamma_i = \sum_{i=1}^{n} \alpha_i A'(\xi_i) \to \infty, \qquad n \to \infty. \tag{16}$$

If α_i and $A'(\xi_i)$ are restricted to be positive, (16) is equivalent to requiring $\sum_{i=1}^{n} \alpha_i$ to diverge. So it follows that the structure of the sequence can be of the form

$$\alpha_n = \frac{a}{n^\eta}, \tag{17}$$

where a is a positive constant and $0 \le \eta \le 1$. It can be shown that for this choice of α_n, and for $c = aA'(\hat{r})$,

$$\frac{E\{\delta_{n+1}\}}{E\{\delta_1\}} = e^{-\frac{cn^{(1-\eta)}}{1-\eta} + cq(\eta)}, \qquad (0 \le \eta < 1) \tag{18}$$

and

$$[A'(\hat{r})]^2 \frac{\sigma_{n+1}^2}{\sigma_\nu^2} = \frac{c}{2n^\eta}, \qquad (0 < \eta < 1), \tag{19}$$

where

$$q(\eta) = \lim_{n\to\infty} \left\{ \frac{n^{1-\eta}}{1-\eta} - \sum_{k=1}^{n} \frac{1}{k^\eta} \right\};$$

e.g., $q(0) = 0$ and $q(1/2) \approx 1.46$. Table I shows the behavior of the statistics for the special cases $\eta = 0$ and $\eta = 1$, where (18) and (19) are not applicable.

Table I—Behavior of statistics for $\eta = 0$ and $\eta = 1$

η	$c = aA'(\hat{r})$	$\frac{\bar{\delta}_{n+1}}{\bar{\delta}_1}$	$\frac{\sigma_{n+1}^2}{\sigma_\nu^2}[A'(\hat{r})]^2$
0	$0 < c < 2$	$(1-c)^n < e^{-cn}$	$\frac{c}{2-c}[1-(1-c)^{2n}] \sim \frac{c}{2-c}$
1	$c > \frac{1}{2}$	$e^{-0.577}/n^c$	$\frac{c^2}{2c-1} \times \frac{1}{n}$
1	1	$e^{-0.577}/n$	$\frac{1}{n}$
1	1/2	$e^{\frac{0.577}{2}}/\sqrt{n}$	$\frac{ln(n)}{4n}$

It is noted from eqs. (17) through (19) and Table I that the choice of a fixed step size ($\eta = 0$) gives the fastest convergence of the mean, $\bar{\delta}_{n+1}$, but results in a finite variance, σ^2_{n+1}, as $n \to \infty$. On the other hand, a variable, progressively smaller step size ($\eta \neq 0$) gives a slower convergence of the mean, but results in a variance approaching zero as $n \to \infty$. Thus, a fixed step size should be used if the measurement error variance, σ_ν^2, is very small, and a variable step size should be used if the variance is large. Actually, when finite-precision arithmetic is employed, the choice of a progressively smaller step size can lead to large errors.[19] Thus, in our particular application where the measurement error can be made small, and where the use of finite-precision arithmetic is necessary, a fixed step size is more suitable.

We note that our algorithm, (9), is based on the polar representation of the data symbols, while the hardware implementation of Fig. 1 is based on the rectangular representation. Thus, the linearizing processor is required to convert back and forth between the two representations. One could avoid this conversion by replacing (9) by the rectangular-based algorithm

$$x_{n+1} + iy_{n+1} = x_n + iy_n - (\alpha_n + i\beta_n)[u_n + iv_n - G(a + ib)].$$

Unfortunately, however, the convergence of this algorithm is not guaranteed, even for some well-behaved amplifier characteristics.

IV. SIMULATIONS

Here we present the results of computer simulations of the algorithm, (9), with fixed step sizes and finite-precision arithmetic. The precision is limited by the finite number of bits of the D/A and A/D converters (Fig. 1). As an example, we consider a TWT amplifier with normalized amplitude and phase nonlinearities of the form[17]

$$A(r) = \frac{2r}{1 + r^2}, \tag{20a}$$

$$\Phi(r) = 60^\circ \frac{r^2}{1 + r^2}, \tag{20b}$$

which are sketched in Fig. 3. Note that at saturation, $r = 1$, $A(r) = 1$, and $\Phi(r) = 30^\circ$. Figure 4 shows the severe distortion of the output constellation obtained with such an amplifier for a 64-QAM input signal driven with its corner point at saturation.

Figures 5, 6, and 7 show the simulated results of the output signal constellations after the application of (9) for three different cases (explained below). In all cases the amplifier drive is maintained at saturation. The four quadrants in each figure represent different combinations of the numbers of bits of the D/A and A/D converters, as indicated in Table II.

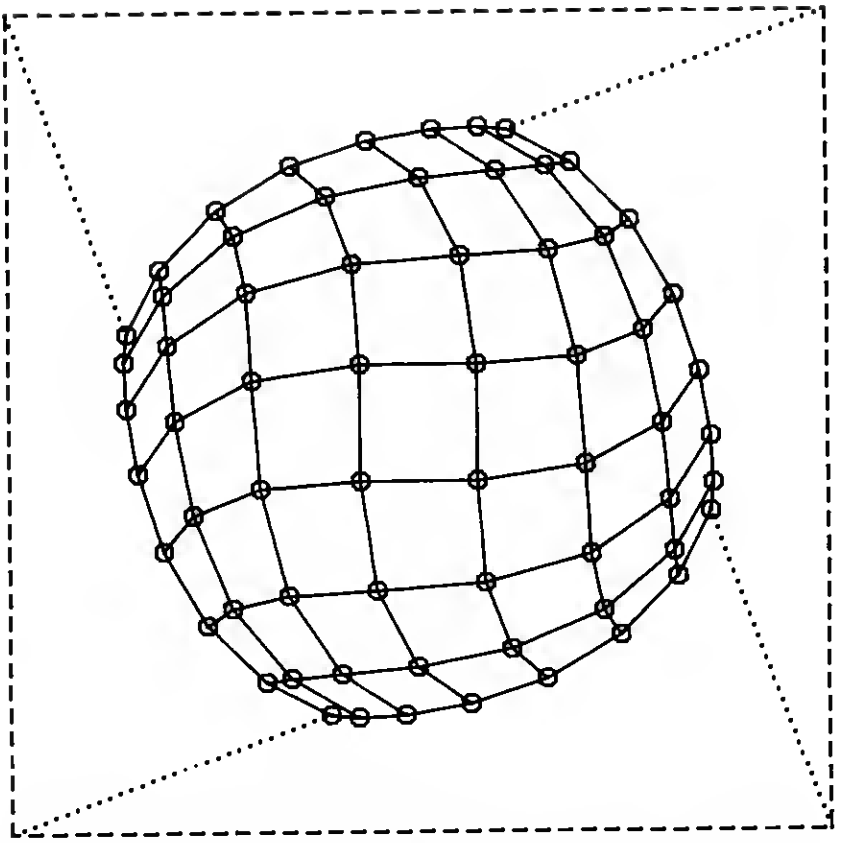

Fig. 4—The distortion of the signal constellation obtained with the amplifier of Fig. 3 for a 64-QAM input signal with its corner points at saturation.

Figure 5 corresponds to the case of no measurement error, i.e., $\nu_n = \mu_n = 0$ in (6). The step sizes used in (9) are $\alpha_n = 0.5$ and $\beta_n = 1.0$. Since the normalized small-signal gain, $A'(r)$, of the amplifier is about 2, the choice of $\alpha_n = 0.5$ results in a value for c of about 1. This results in the fastest convergence of (9a), as can be seen from the first row of Table I. Similarly, the choice of $\beta_n = 1.0$ results in the fastest convergence of (9b) since that equation is linear in θ. The initial guesses of r and θ for each constellation point in Fig. 5 were chosen at random, i.e., from a blind start. The results indicated in the figure are those after 25 iterations for each constellation point. The point scatter shown is entirely due to the finite resolution of the D/A and A/D converters since no measurement errors were assumed.

It is clear from Fig. 5 that the use of 8 bits for both the D/A and A/D converters (fourth quadrant) gives quite an acceptable performance for 64 QAM. The use of 9 bits for each converter (first quadrant)

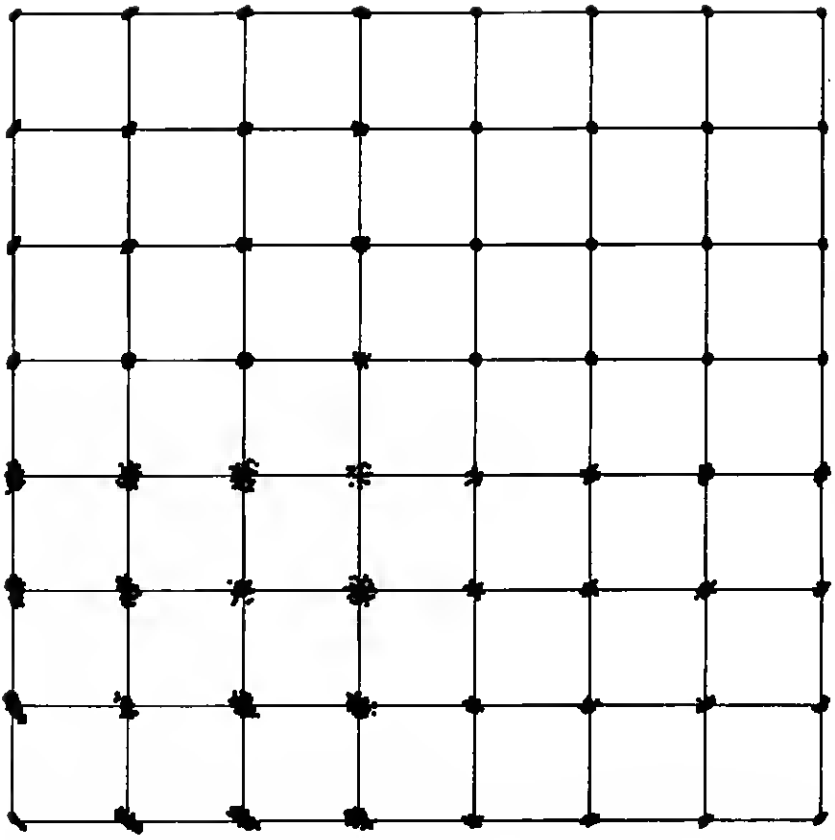

Fig. 5—Simulated results of the output signal constellation after 25 iterations with no measurement errors, and for step sizes $\alpha_n = 0.5$ and $\beta_n = 1.0$. The number of bits of the D/A and A/D converters are different in each quadrant as indicated in Table 2.

results in an almost perfect output constellation. In general, for L^2-QAM, where $L = 2^M$, D/A and A/D converters with $(M + 5)$ bits are needed for acceptable performance, and $(M + 6)$ or more bits are needed for almost perfect performance.

In Fig. 6, the step sizes employed are $\alpha_n = 0.5$ and $\beta_n = 1.0$, as in Fig. 5. However, a measurement error was introduced that is equivalent to a 30-dB signal-to-noise ratio at the corner points of the constellation. With the normalization used for $A(r)$ in (20a), this noise corresponds to $\sigma_\nu^2 = A^2(r)\sigma_\mu^2 = 0.0005$, where σ_ν^2 and σ_μ^2 are the variances of the errors ν_n and μ_n defined in (6). It is clear from Fig. 6 that such a level of noise, in combination with the large step sizes employed, gives unacceptable results.

In Fig. 7, the same noise level as that of Fig. 6 is employed. However, the step sizes were reduced by a factor of 10, i.e., $\alpha_n = 0.05$ and $\beta_n =$

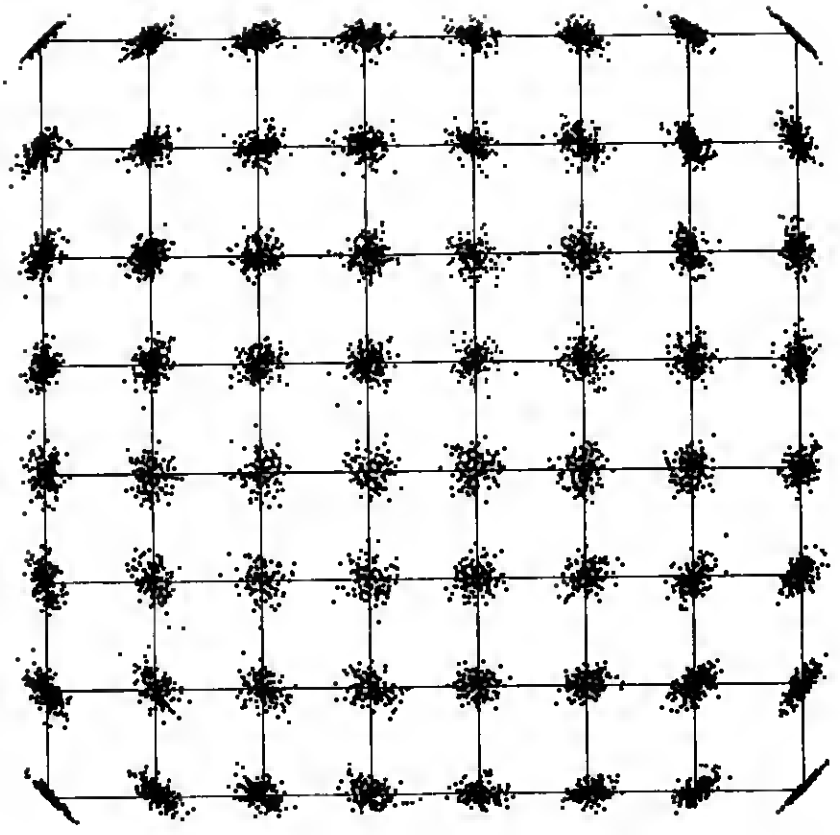

Fig. 6—Same as Fig. 5, but with a measurement error equivalent to 30-dB of signal-to-noise ratio at the corner points of the constellation.

0.1, resulting in a greatly improved performance. About 100 steps of iteration were needed in this case to reach convergence. Note that in spite of the measurement noise, the performance in the third quadrant of Fig. 7 is better than the corresponding performance in Fig. 5, where no noise is present. This is due to the reduced step sizes, and to the fact that the noise tends to smooth out quantization errors.

V. SUMMARY AND CONCLUSIONS

We have proposed and analyzed a transmitter-based, adaptive linearizer, which automatically compensates for power amplifier nonlinearity in digital radio systems employing multilevel quadrature amplitude modulation. The linearizer utilizes a real-time, data-directed recursive algorithm for predistorting the signal constellation. The algorithm is robust and results in rapid convergence, even from a blind

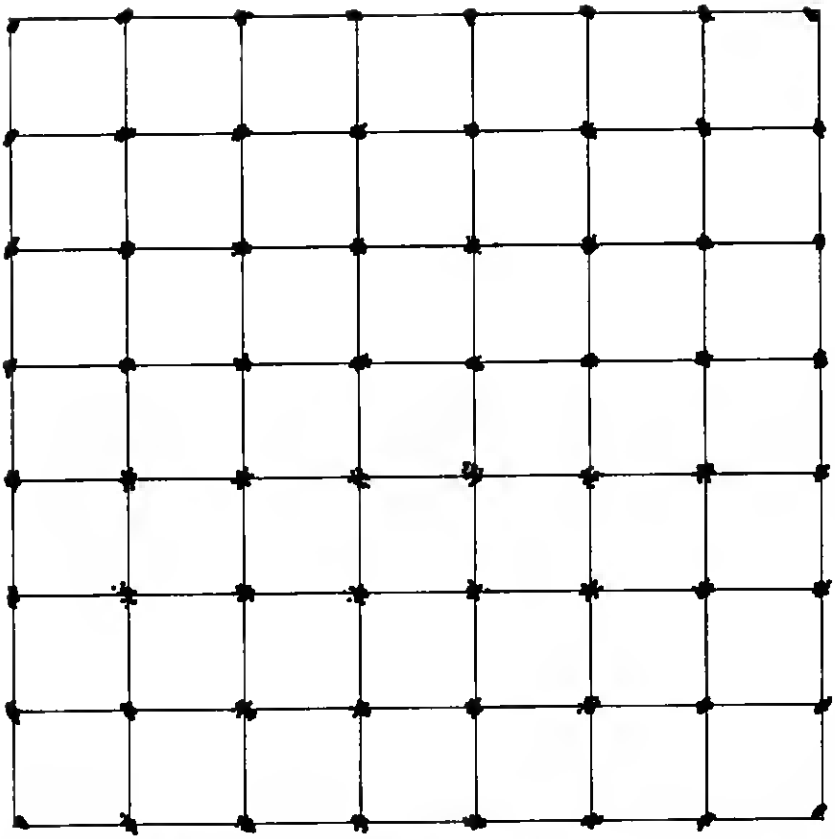

Fig. 7—Same as Fig. 6, but with the step sizes reduced by a factor of 10, i.e., $\alpha_n = 0.05$ and $\beta_n = 0.1$. About 100 iteration steps were needed for convergence.

Table II—Number of bits of the D/A and A/D converters for the four quadrants of Figs. 5, 6, and 7

Quadrant Number	Number of Bits of the D/A Converter	Number of Bits of the A/D Converter
1	9	9
2	9	7
3	8	6
4	8	8

start. The digital nature of the linearizer allows both the signal constellation and the average transmitted power to be changed through software.

The proposed linearizer is only suitable for amplifiers with essen-

tially memoryless and single-valued nonlinearities. Consequently, pulse shaping is not permitted before amplification. In our approach the task of pulse shaping is relegated to the combination of the transmit RF filter, a receiver-based filter, and an automatic equalizer. The latter is presumed to be required anyway to deal with multipath fading, especially for signals having a large number of levels.

Our principal conclusion is that high-power RF amplifiers can operate at saturation, where they are most efficient, provided that an adaptive predistortion linearizer is used. We have demonstrated that such a system is feasible and have provided a theory and a methodology for assessing its performance.

REFERENCES

1. G. J. Foschini and J. Salz, "Digital Communications over Fading Radio Channels," B.S.T.J., *62*, No. 2, Part 1 (February 1983), pp. 429–56.
2. R. P. Hecken and R. C. Heidt, "Predistortion Linearizer of the AR6A Transmitter," ICC '80 Conf. Rec., *2* (June 1980), pp. 33.I.1–6.
3. T. Nojima and Y. Okamato, "Predistortion Nonlinear Compensator for Microwave SSB-AM System," ICC '80 Conf. Rec., *2* (June 1980), pp. 33.2.I–6.
4. A. Egger, M. Horn, and T. Vien. "Broadband Linearization of Microwave Power Amplifiers," Proc. of the 10th European Microwave Conf., September 1980, pp. 490–4.
5. C. Brenson, M. Palazo, and R. Neyer, "Linearizing T.W.T. Amplifiers in Satellite Transponders—System Aspects and Practical Implementation," Proc. of the AIAA 8th Commun. Satellite Conf., April 1980, pp. 80–9.
6. G. Sato, H. Shibazaki, T. Asai, and T. Kurokawa, "A Linearizer for Satellite Communications," ICC '80 Conf. Rec., *2* (June 1980), pp. 33.3.1–5.
7. G. Satoh and T. Mizuno, "Impact of a New TWTA Linearizer Upon QPSK/TDMA Transmission Performance," IEEE J. Select. Areas in Comm., special issue on Digital Satellite Communications, *SAC-1*, No. 1 (January 1983), pp. 39–45.
8. D. D. Falconer, "Adaptive Equalization of Channel Nonlinearities in QAM Data Transmission Systems," B.S.T.J., *57*, No. 7 (September 1978), pp. 2589–611.
9. S. Benedetto and E. Biglieri, "Nonlinear Equalization of Digital Satellite Channels," IEEE J. Select Areas in Comm., special issue on Digital Satellite Communications, *SAC-1*, No. 1 (January 1983), pp. 57–62.
10. W. J. Weber, III, "The Use of TWT Amplifiers in *M*-Ary Amplitude and Phase-Shift Keying Systems," ICC '75 Conf. Rec., *3* (June 1975), 36.17–21.
11. R. C. Davis and W. Boyd, "Adaptive Predistortion Technique for Linearizing a Power Amplifier for Digital Data Systems," U.S. Patent 4,291,277, issued September 22, 1981.
12. T. L. Osborne and P. D. Karabinis, unpublished work.
13. L. J. Greenstein and D. Vitello, "Required Transmit Filter Bandwidth in Digital Radio Systems," IEEE Trans. Comm., *COM-29*, No. 9 (September 1981), pp. 1405–8.
14. H. Wang and C. Ren, private communications.
15. J. K. Plourde and C. Ren, "Application of Dielectric Resonators in Microwave Components," IEEE Trans. Microwave Theory Tech., *MTT-29*, No. 8 (August 1981), pp. 754–70.
16. A. L. Berman and C. H. Mahle, "Nonlinear Phase Shift in Traveling-Wave Tubes as Applied to Multiple Access Communications Satellites," IEEE Trans. Comm. Tech., *COM-18*, No. 1 (February 1970), pp. 37–48.
17. A. A. M. Saleh, "Frequency-Independent and Frequency-Dependent Nonlinear Models of TWT Amplifiers," IEEE Trans. Comm., *COM-29*, No. 11 (November 1981), pp. 1715–20.
18. A. E. Albert and L. A. Gardner, Jr., "Stochastic Approximation and Nonlinear Regression," Research Monograph No. 42, Cambridge, MA: MIT Press, 1967.
19. R. D. Gitlin, J. E. Mazo, and M. G. Taylor, "On the Design of Gradient Algorithms for Digitally Implemented Adaptive Filters," IEEE Trans. Circuit Theory, *CT-20*, No. 2 (March 1973), pp. 125–36.